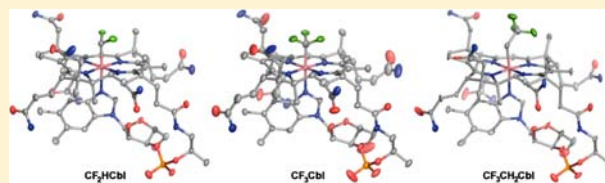


Trans and Cis Effects of Axial Fluoroalkyl Ligands in Vitamin B₁₂ Analogues: Relationship between Alkyl- and Fluoroalkyl-CobalaminsLucio Randaccio,^{†,§} Giovanna Brancatelli,[†] Nicola Demitri,^{†,‡} Renata Dreos,[†] Neal Hickey,[†] Patrizia Siega,[†] and Silvano Geremia^{*,†}[†]Department of Chemical and Pharmaceutical Sciences, University of Trieste, 34127 Trieste, Italy

S Supporting Information

ABSTRACT: CF₂HCbl, CF₃Cbl, and CF₃CH₂Cbl have been synthesized and characterized in solution by ¹H NMR and UV-vis spectroscopy, and their X-ray crystal structures have been determined using synchrotron radiation. The structure of CF₃CH₂Cbl is reported for the first time, whereas those of CF₂HCbl and CF₃Cbl are re-examined to obtain more precise structural data. Comparison of the structural data obtained with the alkylcobalamin analogues, MeCbl and EtCbl, indicates that the Co–C and Co–NB3 bond lengths are shorter in the fluoroalkylcobalamins. The structural data of the fluoroalkylcobalamins previously reported in the literature had been conflicting in this regard. Thus, a much less dramatic shortening of the two axial bonds was found for CF₃Cbl, whereas in the case of CF₂HCbl, the Co–NB3 bond length is shorter than in MeCbl. Direct comparison of the structures of CF₃CH₂Cbl and EtCbl indicates a large distortion of the axial fragment in the former case that can be attributed to steric effects. A number of previously reported correlations of the effect of the β-ligand on the structure and properties of cobalamins are re-examined in light of the present results. Particular emphasis is placed on the axial fragment. This analysis substantially confirms and, with the new data reported here, adjusts and expands the data set for correlations between trans and cis influences of the β-ligand of cobalamins and their structure (Co–X and Co–NB3 distances and corrin fold angle) and properties (UV-vis spectra, NMR spectra, and pK_{base-off}).



1. INTRODUCTION

Cobalamins, X(R)Cbl, are corrinoids of the structural formula shown in Figure 1a. The axial ligand is denoted by R when it is bonded to Co through a Co–C bond. Vitamin B₁₂ or cyanocobalamin, CNCbl, is enzymatically converted in vivo to the two B₁₂ cofactors: methylcobalamin (MeCbl, R = methyl) and adenosylcobalamin (AdoCbl, R = 5-deoxyadenosyl). All known reactions of B₁₂-dependent enzymes involve the making and breaking of the Co–C bond.^{1,2} For AdoCbl, the accepted enzymatic mechanism involves homolytic Co–C bond cleavage, whereas heterolytic cleavage is believed to occur for MeCbl. The Co–C bond is dramatically influenced by the interaction of the coenzyme with the peptide chain of the active site. For example, this interaction is responsible for an enhancement of more than 12 orders of magnitude of the Co–C bond homolysis rate in AdoCbl when it is bound to the apoenzyme.³ The factors that determine such a rate enhancement have not yet been fully elucidated and remain the topic of numerous studies in which the behavior of the axial R–Co–NB3 fragment (Figure 1) is of particular interest. Furthermore, the binding of the cofactors to the apoenzyme often involves the displacement of the benzimidazole moiety from cobalt. Understanding why this occurs in some enzymes and not in others is further reason to investigate the properties of the axial fragment in cobalamins. In addition to the direct studies on cobalamins,^{1,4} a significant contribution to the understanding of the properties of the cofactor axial bonds derives from the

extensively studied B₁₂ models, the cobaloximes, LCo(DH)₂R (Figure 1b).^{5,6} Such studies have revealed interesting observations when hydrogen atoms of the R group are substituted with highly electronegative fluorine. Thus, comparison of several alkylcobaloximes with their fluoroalkylcobaloximes analogues clearly showed that partial or total fluorination of an alkyl group induces a shortening of both the axial Co–C and Co–N distances.⁷ This result was interpreted in terms of differences in steric and electronic properties between an alkyl and the corresponding fluoroalkyl group.⁸ In fact, because of their lower electron-donating ability with respect to their alkyl analogues, fluoroalkyl fragments are less powerful trans-influencing ligands, thereby inducing a shorter Co–N axial bond with respect to that trans to the corresponding alkyl. However, the electron-withdrawing ability of the fluoroalkyl ligands also induces a shortening of the Co–C bond, which is the opposite of the expected influence resulting from the increase in the bulk, which should lengthen this bond. Thus, a shortening of up to about 0.05 Å was observed for both axial bonds, depending on the nature of the R ligand. Similar behavior was observed in the other B₁₂ simple models, the iminocobaloximes⁴ (Figure 1b). These structural differences nicely correspond to those found when NMR spectroscopic and kinetic data of a limited number of fluoroalkylcobaloximes

Received: July 5, 2013

Published: November 12, 2013

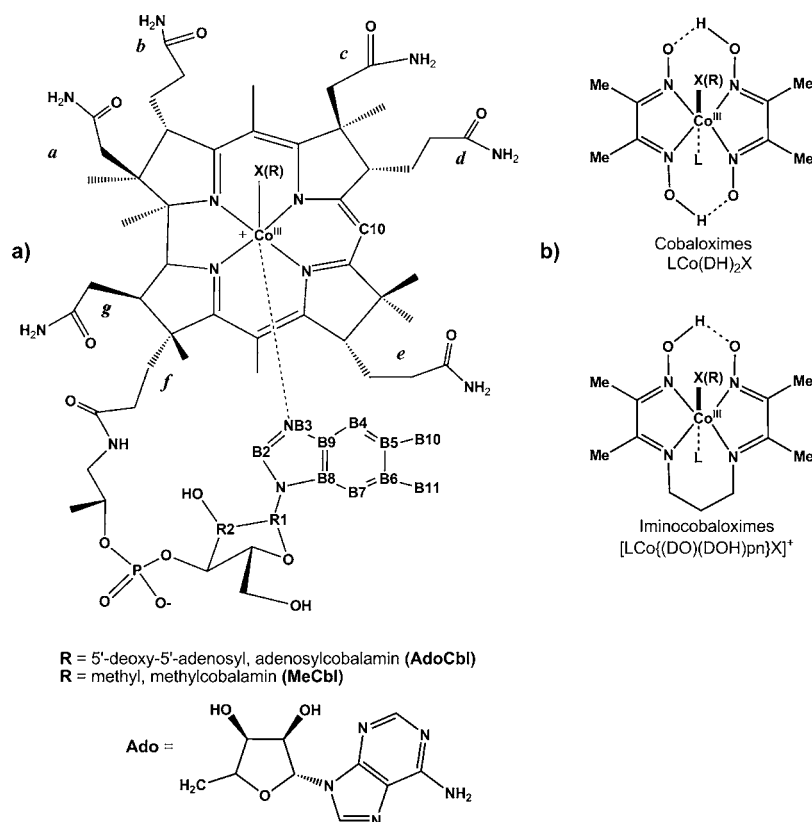


Figure 1. Scheme of (a) cobalamins (Cbl), with the conventional numbering for benzimidazole C atoms and labeled amide side chains, (b) cobaloximes, $\text{LCo}(\text{DH})_2\text{X}$, and iminocobaloximes, $[\text{LCo}\{(\text{DO})(\text{DOH})\text{pn}\}\text{X}]^+$. X is generally denoted by R when the ligand is an alkyl group. The two cofactors of B_{12} enzymes (AdoCbl and MeCbl) are specified. In vitamin B_{12} , or cyanocobalamin, $\text{X} = \text{CN}$.

were compared with those of alkylcobaloximes.⁸ On the basis of these results, similar findings should be expected when fluoroalkylcobalamins are compared with alkylcobalamins.

Very limited information is available on the structure and properties of fluoroalkylcobalamins. Several decades ago, some fluoroalkylcobalamins were obtained from a variety of Freons by a modification of the standard procedure used for the synthesis of alkylcobalamins.⁹ This early study showed that there is a linear relationship between the electronegativity of the R ligand and the stability of the Co–C bond to light in the R order $\text{CF}_3 > \text{CFCl}_2 > \text{CF}_2\text{H} > \text{Me}$. This trend was attributed to stronger Co–C bonds in fluoroalkylcobalamins with respect to those in MeCbl. Subsequently, some fluoroalkylcobalamins were studied and compared with alkylcobalamins, principally by NMR spectroscopic^{10–12} and kinetic and thermodynamic studies.¹³

Deeper knowledge of fluoroalkylcobalamins could be also useful in view of their possible role in the emerging field of ^{19}F MRI diagnostics.^{14,15} It is well-known that rapidly proliferating cells, such as tumor cells, require high amounts of cobalamin. This observation has given considerable potential to the use of vitamin B_{12} analogues as imaging agents for the diagnosis of these cell types or as therapeutic drugs exploiting the conjugated groups with growth-blocking or cytotoxic properties.¹⁶ Thus, fluorinated cobalamins could be also investigated as potential contrast agents for diagnostic applications. Furthermore, a β -axial-ligand-substituted vitamin B_{12} has been recently investigated as a promising antivitamin B_{12} ¹⁷ that would be taken up by the vitamin B_{12} transport proteins in mammals without subsequent conversion into active B_{12} cofactors.

To our knowledge, only the X-ray structures of CF_2HCbl ¹⁸ and CF_3Cbl ¹⁹ have been reported for fluoroalkylcobalamins. However, on the basis of the observations of the B_{12} models, these structures showed unexpected structural features. Thus, in the case of CF_3Cbl , a relatively large shortening ($\sim 0.1 \text{ \AA}$) was reported for both axial distances with respect to those for MeCbl. In the case of CF_2HCbl , the Co–C bond is shorter ($\sim 0.04 \text{ \AA}$) than the Co–Me bond in MeCbl, but, surprisingly, the Co–NB3 bond is longer ($\sim 0.03 \text{ \AA}$) than its MeCbl analogue. These anomalies prompted us to determine the X-ray structure of $\text{CF}_3\text{CH}_2\text{Cbl}$ and to reanalyze those of the previously reported CF_2HCbl and CF_3Cbl . To have very precise structural determinations of fluoroalkyl- B_{12} derivatives, synchrotron radiation was used. From a wider perspective, it is important to note that (not only in relation to cobaloximes and cobalamins but for organometallic complexes in general) structural trends and structure/activity correlations for fluorine-substituted alkyl ligands are not wholly understood, and the explanation of the bonding remains a matter of debate.^{20–22} Here, we report the preparation and crystal structure analysis of $\text{CF}_3\text{CH}_2\text{Cbl}$ (1), CF_3Cbl (2), and CF_2HCbl (3) on the basis of synchrotron data collected at 100 K. The ^1H NMR and UV–vis spectra of the fluoroalkylcobalamins are also reported and discussed together with those reported for a number of cobalamins. Finally, on the basis of available precise structural data for cobalamins, a number of previously reported features, structural aspects of the axial fragment, structure–property correlations, and comparisons between cobaloximes and cobalamins, are re-examined and expanded in light of the new data reported here.

2. EXPERIMENTAL SECTION

2.1. General Procedures and Chemicals. All manipulations involving alkylcobalamins were performed in the dark. HOCbl-HCl, SP Sephadex resin, NaBH₄, acetone, methanol, and D₂O were purchased from Sigma-Aldrich. CF₃CH₂I was provided by Acros. CF₂HI and CF₃I were purchased from Fluorochem. All reagents and solvents were analytical grade and used without further purification. UV-vis spectra of RCbl (0.05–0.5 mM in H₂O at pH 7.0) were recorded with an UVIKON 941 PLUS spectrophotometer at 25 °C. To avoid the process of photolysis, the solutions for UV-vis spectra were prepared in the dark, and the spectra were recorded immediately. A rough estimation of cobalamin concentration was obtained by evaluating the concentration of H₂Ocbl produced by photolysis of the starting samples. ¹H NMR spectra were recorded using a JEOL EX-400 instrument (¹H at 400 MHz) or a Varian 500 Inova instrument (¹H at 499 MHz) in D₂O at pD 7.0 using DSS (2,2-dimethyl-2-silapentane-5-sulfonate sodium salt) as the reference. The ¹H NMR spectra indicated the absence of significant amounts of byproducts (Figure S1). Electrospray mass spectra were recorded in positive mode with a Bruker ESQUIRE 4000 mass spectrometer.

2.2. Syntheses. CF₃CH₂Cbl (1). **1** was synthesized via a previously reported procedure²³ with some modifications. HOCbl-HCl (0.250 g, 1.81 × 10⁻⁴ mol) was dissolved in 5 mL of a MeOH/H₂O mixture (3:1). The solution was deaerated several times, and NaBH₄ (0.100 g dissolved in a few drops of H₂O) was added under a nitrogen atmosphere with continuous stirring. After 5 min, an excess of CF₃CH₂I was added (0.38g, 1.81 × 10⁻³ mol), and the solution was further stirred under nitrogen for 20 min. After addition of 50 mL of acetone, a solid was collected by filtration and then dissolved in 2 mL of H₂O. After adjusting the pH to ca. 2 with aqueous HCl, the solution was applied to a SP Sephadex column and eluted with water to separate unreacted aquacobalamin. The eluted solution was evaporated under vacuum, and a red solid was obtained. Yield: 0.131 g, 51.2%. ESI-MS (174.2 V, H₂O): *m/z* calcd (%) for C₆₄H₉₀CoF₃N₁₃O₁₄P (exact and most abundant mass), 1411.6; found, 1412.3 (S) [M + H⁺], 1434.6 (27) [M + Na⁺], 1351.6 (100) [M - CF₃CH₂ + Na⁺]. ¹H NMR (ppm, aromatic region): δ 7.19 (s, 1H), 6.98 (s, 1H), 6.32 (s, 1H), 6.28 (d, 1H), 5.97 (s, 1H).

CF₃Cbl (2). **2** was prepared as reported above with some modifications. After the reduction of aquacobalamin, gaseous CF₃I was bubbled through the reaction mixture for 10 min, and then 50 mL of acetone was added. A short alkylation time was used to minimize the formation of CF₂HCbl, which has been reported for long alkylation times using a similar procedure.²⁴ A solid was collected by filtration and dissolved again in a minimal amount of H₂O. AgNO₃ was added to convert the possibly formed ICbl to aquacobalamin. After filtration, the pH was adjusted to ca. 2 with aqueous HCl, and the solution was applied to a SP Sephadex column and eluted with water. The eluted solution was evaporated under vacuum, and a red solid was obtained. Yield: 0.059 g, 23.3%. ESI-MS (173.4 V, H₂O): *m/z* calcd (%) for C₆₃H₈₈CoF₃N₁₃O₁₄P (exact and most abundant mass), 1397.6; found, 1398.7 (100) [M + H⁺], 1420.7 (27) [M + Na⁺], 1351.7 (32) [M - CF₃ + Na⁺]. ¹H NMR (ppm, aromatic region): δ 7.21 (s, 1H), 7.01 (s, 1H), 6.39 (s, 1H), 6.29 (d, 1H), 6.01 (s, 1H).

CF₂HCbl (3). **3** was prepared by a similar procedure as that for CF₃CH₂Cbl using gaseous CF₂HI as the alkylating agent. Yield: 0.085 g, 34.1%. ESI-MS (172.5 V, H₂O): *m/z* calcd (%) for C₆₃H₈₉CoF₂N₁₃O₁₄P (exact and most abundant mass), 1379.6; found, 1380.7 (28) [M + H⁺], 1402.7 (100) [M + Na⁺], 1351.7 (44) [M - CF₂H + Na⁺]. ¹H NMR (ppm, aromatic region): δ 7.21 (s, 1H), 7.01 (s, 1H), 6.33 (s, 1H), 6.29 (d, 1H), 5.97 (s, 1H).

2.3. X-ray Diffraction Studies. X-ray quality crystals were obtained by slow diffusion of acetone or MeOH in aqueous solutions of the RCbls at 4 °C. Crystal structure analysis of CF₃CH₂Cbl (**1**), CF₃Cbl (**2**), and CF₂HCbl (**3**) was based on synchrotron data (XRD1 diffraction beamline of Elettra, Trieste) collected at 100 K with wavelengths of 0.77491, 0.7, and 0.6 Å and refined to 9.35, 7.02, and 6.15% *R*-factor values, respectively (MarCCD detector for CF₂HCbl and Pilatus 2 M detector for CF₃Cbl and CF₃CH₂Cbl). As a general

procedure, the crystal, dipped in *N*-paratone, was mounted in a loop and frozen at 100 K. The diffraction data were indexed and integrated using the XDS package²⁵ for CF₂HCbl and CF₃Cbl and Mosflm²⁶ for CF₃CH₂Cbl and scaled by SCALA^{27,28} for CF₂HCbl and CF₃CH₂Cbl and Aimless^{27,28} for CF₃Cbl. The isomorphous structures were solved by direct methods using Sir2008.²⁹ Fourier analyses and refinements were conducted by the full-matrix least-squares, on the basis of *F*², implemented in SHELXL-97³⁰ using Coot³¹ to build the model. Empirical absorption corrections were applied by the XABS2³² program. The asymmetric unit of CF₂HCbl contains one crystallographically independent CF₂HCbl molecule, nine water molecules (six at full occupancy as well as two at 75% and one at 70% partial occupancy) and four acetone molecules (one at full occupancy as well as one at 80% and two at 70% partial occupancy). The axial CF₂H ligand was found disordered over two positions: the two pairs of fluorine atoms were refined with occupancy of 70 and 30% for each fragment orientation. Moreover, two positions for the carbonyl group in the amidic chain *a* were refined at 60 and 40% of occupancy.

The asymmetric unit of CF₃Cbl consists of one crystallographically independent CF₃Cbl molecule, 12 water molecules (three at full occupancy, three disordered over two positions, 80/20%, 70/30%, and 60/40%, and six with partial occupancy, 85, 50, 30, 25, 25, and 20%) and two acetone molecules (one at full and one at half occupancy). The axial coordination site is partially occupied by a CF₃ ligand and an iodine anion. The occupancies of both ligands were refined at 93 and 7% for CF₃ and I, respectively. Attempts were made to eliminate this inhomogeneity by addition of Ag⁺ to solutions of CF₃Cbl, and diffraction data were collected on several occasions using crystals from different batches. The problem, however, persisted, and the data reported here are the best results obtained. Successively, in the final stages of refinement the occupancy, coordinates and thermal parameters were fixed for the iodine atom. Moreover, one amidic arm was found disordered over two positions, refined at 40 and 60% of occupancy. The asymmetric unit of CF₃CH₂Cbl contains one crystallographically independent CF₃CH₂Cbl molecule, 18 water molecules (nine at full occupancy, two disordered in two positions (25/25% and 25/25%), four at 50%, one at 40%, and two at 25% occupancy) and one methanol molecule. Two positions for the carbonyl oxygen atom in the amidic chain *a* were refined at half occupancy.

In the final refinement, hydrogen atoms were included at calculated positions and all non-hydrogen atoms with full occupancy were treated anisotropically (except for F and I atoms with 30 and 7% of occupancy in the CF₂HCbl and CF₃Cbl crystal structures, respectively). Essential crystal data and refinement details are reported in Table S1. The observed disorder, mainly at the level of solvent molecules, affects the *R*-factor values.

3. RESULTS

3.1. X-ray Structures of CF₂HCbl, CF₃Cbl, and CF₃CH₂Cbl. The ORTEP drawings between the three cobalamins are shown in Figure 2. All three structures are in their usual base-on form with the benzimidazole moiety coordinated to Co in the α -axial position (corrin lower side). The fluoroalkyl ligands coordinate Co in the β -axial position (corrin upper side) through a Co–C bond. The crystal structures and crystal packing observed are in line with previous reports on cobalamins: all three compounds crystallized in the orthorhombic space group *P*2₁2₁ and show type II packing.³³ The corrin fold angles are 15.7° (CF₂HCbl and CF₃Cbl) and 15.0° (CF₃CH₂Cbl). Therefore, as expected, there is high structural similarity among the structures with regard to the conformations of the equatorial corrins, the imidazol ligands, and the amide side chains. However, a clear distinction of the three fluoroalkylcobalamins was possible by superimposition of the structures (Figure 3). In CF₃CH₂Cbl, the CF₃–CH₂ moiety is clearly tilted out of the ideal C–Co–NB3 axis. As

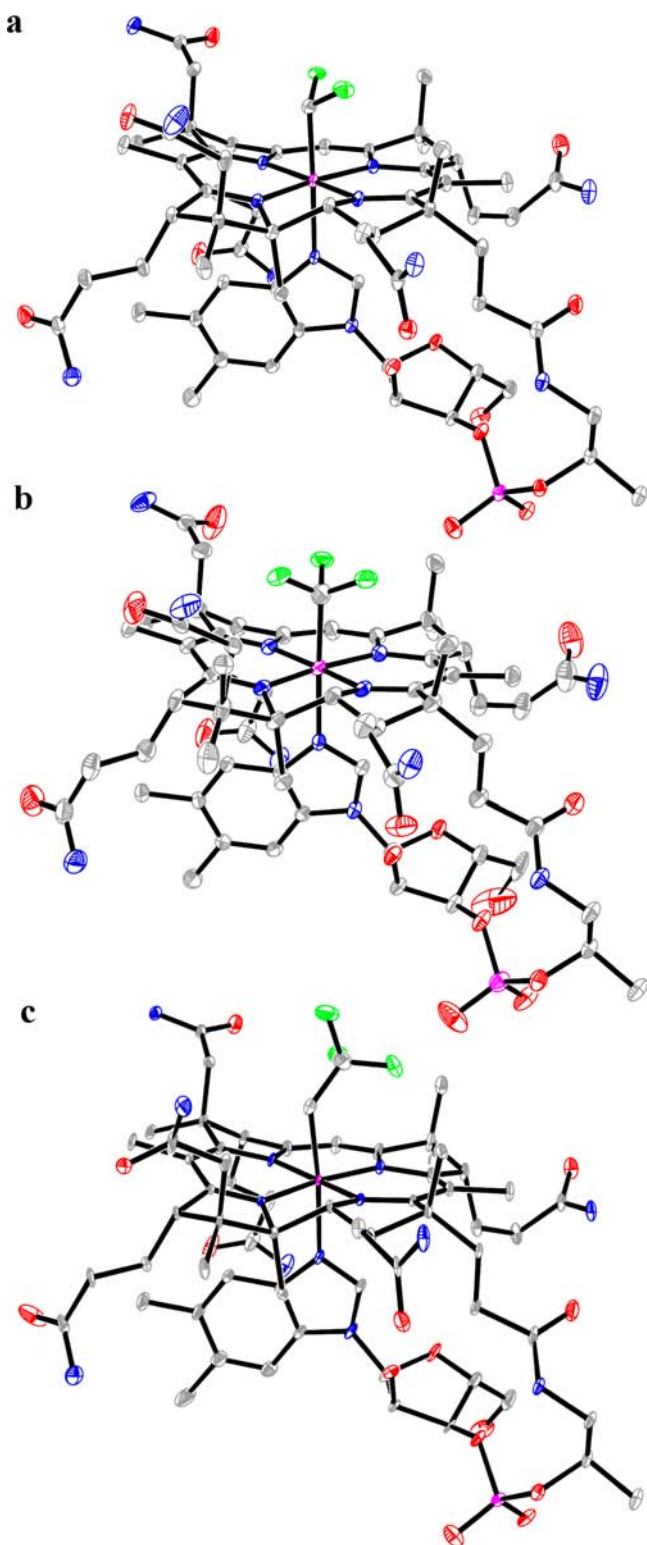


Figure 2. Ortep views of (a) CF_2HCbl , (b) CF_3Cbl , and (c) $\text{CF}_3\text{CH}_2\text{Cbl}$ structures with thermal ellipsoids at 30, 20, and 30% probability levels, respectively.

a consequence, three $\text{C}-\text{Co}-\text{N}_{\text{eq}}$ angles are significantly smaller than 90° ($86.4(2)^\circ$, $87.7(2)^\circ$, and $88.0(2)^\circ$), with the other $\text{C}-\text{Co}-\text{N}_{\text{eq}}$ angle being $97.3(2)^\circ$. The CF_3-CH_2 bond lies almost over one of the equatorial $\text{Co}-\text{N}$ bonds. The distortion of the axial ligand and this orientation with respect to the equatorial corrin, similar to that reported for cobaloxime

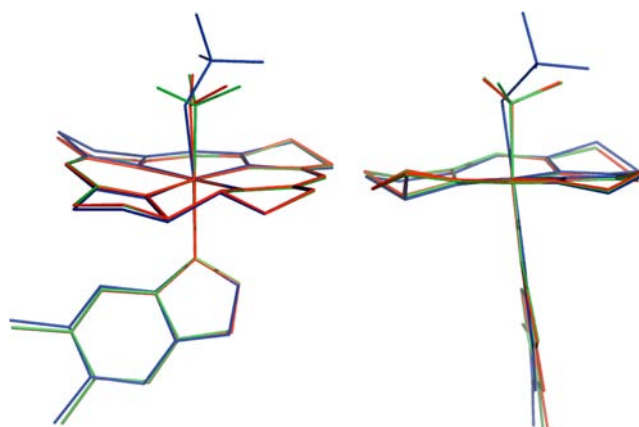


Figure 3. Overlay of the structures CF_2HCbl (red), CF_3Cbl (green), and $\text{CF}_3\text{CH}_2\text{Cbl}$ (blue). To highlight the distortions on the axial fragment geometries, only the equatorial corrin, benzimidazole, and fluoroalkyl ligands are reported.

derivatives,³⁴ is also clearly evident in Figure 2c. Comparison of $\text{CF}_3\text{CH}_2\text{Cbl}$ with the structure of EtCbl ³⁵ indicates that a similar tilt is less evident for the latter structure, as shown by the superimposition of the two structures in Figure 4. This distortion of the geometry may be attributed to steric interaction between the CF_3 group and the equatorial moiety (cis steric influence).

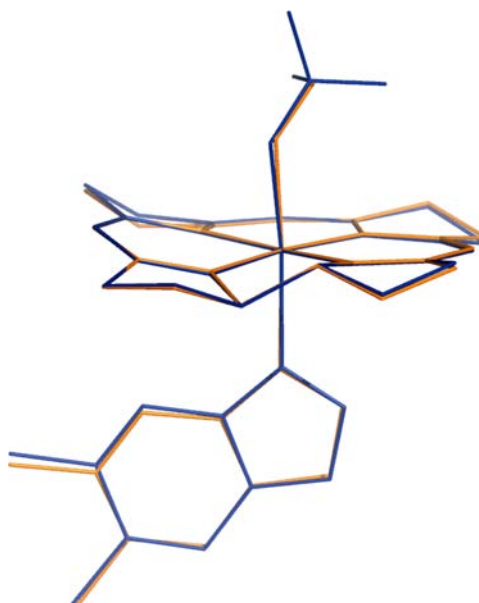


Figure 4. Overlay of the structures of EtCbl (blue, from ref 35) and $\text{CF}_3\text{CH}_2\text{Cbl}$ (yellow). To highlight the distortion of the axial fragment geometry in $\text{CF}_3\text{CH}_2\text{Cbl}$, only the equatorial corrin, benzimidazole, and β -axial ligands are reported.

The axial distances of the fluoroalkylcobalamin structures investigated are reported in Table S2, where they are compared with the cobalamins containing their parent alkyl groups. In the case of CF_2HCbl , the β -axial ligand was found to be disordered over two positions. In both orientations of the CF_2H fragment, differing by a rotation of about 100° around the $\text{Co}-\text{C}$ bond, a $\text{C}-\text{F}$ bond lies almost over one of the equatorial $\text{Co}-\text{N}_{\text{eq}}$ bonds, whereas the other one is orientated between two chelating nitrogen atoms. The two positions for the CF_2H

ligand were refined with 0.7 and 0.3 occupancies; thus, the values reported in Table S2 refer to the conformation with higher occupancy. The $\Delta(\text{Co}-\text{C})$ and $\Delta(\text{Co}-\text{N})$ values in Table S2, that is, the differences in the axial Co–C and Co–N bond distances, respectively, between the related alkyl and the fluoroalkyl derivatives, clearly indicate a significant shortening of both axial bonds in the fluoroalkylcobalamins. Therefore, comparison of the axial fragment in the present structural determination of CF_2HCbl with that of the less precise structure previously reported¹⁸ shows that the axial Co–C distance of 1.938(3) Å does not significantly differ from that of 1.949(8) Å previously reported, whereas the axial Co–N distance of 2.137(2) Å is significantly shorter than that of 2.187(7) Å previously published. Thus, as expected and in contrast to the previous report, the axial Co–N distance in CF_2HCbl is shorter than that in MeCbl . Analogously, comparison of the structural determinations of CF_3Cbl clearly shows that, with respect to MeCbl , the shortening of both axial distances observed for the present, more precise, structural determination is less dramatic than that previously reported,¹⁹ being approximately halved. Similarly, the new structure, $\text{CF}_3\text{CH}_2\text{Cbl}$, exhibits a shortening of both axial distances when compared with EtCbl .³⁵ In $\text{CF}_3\text{CH}_2\text{Cbl}$, the shortening of the Co–C bond with respect to EtCbl corresponds to an increase in the Co–CH₂–C angle of about 5°. This is also found in the corresponding trifluoroethyl simple models (Table S2). Finally, comparison between cobalamins and the corresponding simple models, cobaloximes and iminocobaloximes, clearly shows that the axial fragment has a similar behavior (Table S2). In particular, the Co–C distances are very similar, whereas the axial Co–N distances are significantly shorter (up to 0.1 Å) in the simple models compared to the cobalamins.

3.2. Spectroscopic Characterization of CF_2HCbl , CF_3Cbl , and $\text{CF}_3\text{CH}_2\text{Cbl}$. UV–vis band positions and the chemical shift of the hydrogen atom on C10 in ¹H NMR spectra have both been reported to be sensitive to the electronic influence of the β -axial substituent on the electronic environment of the corrin ring.^{36,37} As such, they may be viewed as probes of the cis influence. With regard to the ¹H NMR spectra, it has been reported that increased electron donation of the β -axial substituent induces a downfield shift of the signal.^{36,37} However, a detailed NMR investigation of a series of cobalamins reported that the H-C10 hydrogen “resonance shifts in an erratic manner, possibly reflecting counteracting influences of changes in electronic density and in anisotropy of both the cobalt atom and the corrin macrocycle”, which suggests that correlation of the position of the H-C10 NMR shift and electronic properties should be re-examined.²³ The results obtained in the present study are consistent with the latter suggestion. Thus, the H-C10 signal, assigned by analogy with data available in the literature,²³ is shifted upfield in $\text{CF}_3\text{CH}_2\text{Cbl}$ ($\delta = 5.97$ ppm) with respect to that reported for EtCbl ($\delta = 6.06$ ppm), whereas it is shifted downfield in CF_3Cbl ($\delta = 6.01$ ppm) and in CF_2HCbl ($\delta = 5.97$ ppm) with respect to MeCbl ($\delta = 5.91$ ppm). This indicates that factors other than electronic influence of the β -axial substituent should be considered in analysis of the position of this signal.

The UV–vis spectra of the three structures reported in the present work are shown in Figure 5. As is the case for all cobalamins, the UV–vis spectra exhibit two main features: the $\alpha\beta$ bands in the region around 450–600 nm and the γ band around 350 nm. The complexity of the UV–vis spectra of

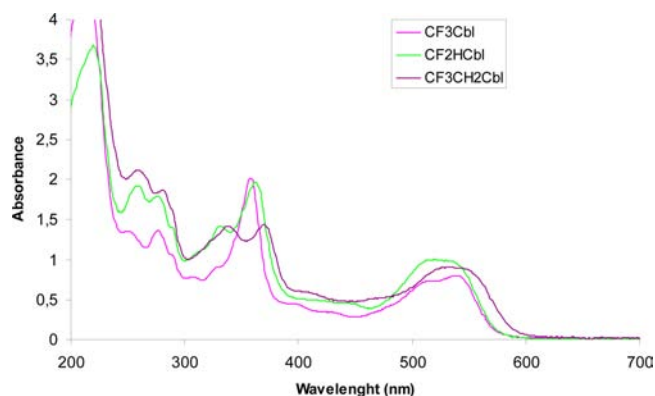


Figure 5. UV–vis spectra of aqueous solutions of CF_2HCbl , CF_3Cbl , and $\text{CF}_3\text{CH}_2\text{Cbl}$ (approximate concentration 1×10^{-4} M).

cobalamins makes it difficult to unambiguously determine the band positions. However, in general, the spectra of cobalamins with a prominent γ band have been referred to as typical, whereas those where that band is less well-defined have been termed atypical.³ On this basis, the spectrum of CF_3Cbl is typical, whereas that of $\text{CF}_3\text{CH}_2\text{Cbl}$ may be described as atypical. The spectrum of CF_2HCbl appears as a transition between the two types, displaying an intense γ band with a side-peak. Marques et al.³⁸ have analyzed the γ region for a number of cobalamins, including both typical (H_2OCbl^+ and NO_2Cbl) and atypical spectra ($\text{S}_2\text{O}_3\text{Cbl}^-$, SO_3Cbl^- , SeCNCbl , and MeCbl) and found that it could be modeled by three Gaussian functions in all cases. The authors concluded that there is no fundamental difference between the typical and atypical spectra of the six cobalamins investigated because the apparent differences are due to the moving apart of the components of the γ band as a consequence of the increase in donation of electron density from the axial ligand field. However, theoretical considerations have indicated that the spectra “types” do in fact differ on the basis of a different Z_{eff} of the metal because of electron donation of the β -ligand and consequent changes in orbital energies.³⁹ In any case, the position of the γ band (and indeed the $\alpha\beta$ -absorption envelope) has been shown to depend on the electron-donating power of the X ligand: the more electron donating the axial X ligand is, the more the γ band moves to longer wavelengths, and, as such, the band positions may still be considered as a probe of the cis influence. Our results (λ_{max} for γ band in CF_3Cbl , CF_2HCbl , and $\text{CF}_3\text{CH}_2\text{Cbl}$ was observed at 358, 362, and 370 nm, respectively) fit well with this description because the γ band moves to longer wavelengths with an increase of the donor strength of the axial ligand ($\text{CF}_3 < \text{CF}_2\text{H} < \text{CF}_3\text{CH}_2$). A similar behavior has been reported for another RCbl series (R = CN, ethynyl, vinyl, and methyl).⁴⁰ Interestingly, the shape of the γ band also changes from typical to atypical progressing from CF_3 to CF_3CH_2 , which follows the donor-strength order. A similar change can also be clearly observed in spectra reported in this early work.⁴⁰

Marques et al.³⁸ have reported the plot of the apparent position of the γ band maximum (a measure of the above-described cis influence³) against the Co–NB3 distance (a measure of the trans influence⁶). Evidence for a correlation, albeit weak, between the cis and trans influences was found ($r^2 = 0.58$). On this basis, we have extended the correlation to a significantly larger number of cobalamins, including the structures described here. The γ band maxima and corresponding Co–NB3 distances (esd values ≤ 0.005 Å) are reported in

Table 1. The plot of the γ band maximum against the Co–NB3 distance of Figure 6 shows a correlation with r^2 of 0.73 (full

Table 1. Position of γ Band (nm) in the UV–Vis Spectra and Co–NB3 Distances (Å) for Various RCbls

R	γ band		Co–NB3	
	maximum	ref	distance	ref
Et	375	50	2.232	35
Me	373	38	2.157	51
CN [−]	360.5	50	2.046	51
N ₃ [−]	358	50	1.999	52
OH [−]	357	50	1.985	53
H ₂ O	350	50	1.925	54
Cl [−]	352	50	1.990	52
NO ₂	353	38	2.008	38
CF ₂ H ^a	362	present work	2.137	present work
CF ₃ ^a	358	present work	2.099	present work
CH ₂ CF ₃	370	present work	2.143	present work
S ₂ O ₃ ^{2−}	367	50	2.078	38
thiourea	366	50	2.032	41
SO ₃ ^{2−}	364	50	2.134	55
SeCN [−]	369	38	2.100	38

^aThe λ_{\max} values for the γ band observed by us slightly differ from those reported in ref 9 (362 nm for CF₃Cbl and 357 nm for CF₂HCbl), but for CF₂HCbl, λ_{\max} agrees with ref 18.

line), significantly better than that previously found. Thus, the decrease in Co–NB3 distance observed on fluorine substitution is reflected in the shift of the γ band maximum to shorter wavelength. However, it is of interest to note that when

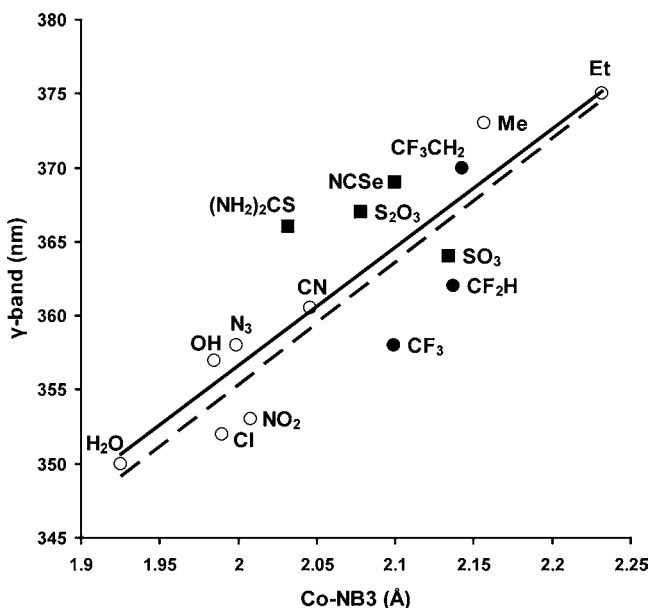


Figure 6. Plot of the position of the γ band against Co–NB3 distances for the cobalamins indicated in Table 1. The full line indicates the linear regression analysis of all of the data plotted using the equation γ band = 79.892 Co–NB3 + 196.84, $r^2 = 0.730$ ($n = 15$). The dashed line indicates the linear regression analysis of the data excluding X groups with S and Se donor ligands using the equation γ band = 82.769 Co–NB3 + 189.81, $r^2 = 0.839$ ($n = 11$). The fluoroalkylcobalamins reported in the present work are evidenced by filled circles. X groups with S or Se donor ligands are evidenced by filled squares.

cobalamins with axial Co–S and Co–Se bonds are excluded the correlation significantly improves to an r^2 value of 0.84 (broken line in Figure 6). It should be recalled that the normal trans influence occurs in cobalamins with X groups having S donors, in contrast with the inverse trans influence observed in cobalamins with C donor axial ligands.⁶ DFT calculations on the corrin model^{41,42} attributed such a difference to a different trend of the positive charge on Co in the two cases. In other words, there is a different transmission of the electronic charge from the X ligand to cobalt in cobalamins with S and C donor axial ligands.

4. DISCUSSION

As outlined in the introduction, the behavior of the axial fragment is of fundamental importance in understanding the activity behavior of cobalamins, and the extensively studied B₁₂ models, the cobaloximes, have furnished an important contribution to the understanding of the axial fragment. Furthermore, fluoroalkyl substituents generally show unusual behavior from the point-of-view of structure/reactivity correlations. Thus, in this section, the data will be presented and discussed from these perspectives, and a number of previously reported features, structural aspects of the axial fragment, structure–property correlations, and comparisons between cobaloximes and cobalamins, will be re-examined and expanded in light of the new data reported here.

4.1. Geometry of the Axial Fragment. Comparison between the axial distances in fluoroalkylcobalamins with those in the parent alkylcobalamins shows a significant shortening in the former (Table S2). This is in agreement with a previous finding⁶ that cobalamins containing a Co–C(R) bond display the so-called inverse trans influence, normally observed when the alkyl R ligands have increasing bulk and electron-donating ability. That is, both axial bonds lengthen or shorten when the bulk and the donating ability of the upper R ligand increase or decrease, respectively. A linear correlation ($r^2 = 0.85$), shown in Figure 7, was obtained by plotting Co–C against Co–NB3 distances for a number of alkylcobalamins and fluoroalkylcobalamins, whose axial Co–NB3 distances have esd values < 0.005 Å. Details of the structural data used are contained in Table S3. In Figure 7, the fluoroalkylcobalamins reported in the present work are evidenced by filled circles, whereas filled squares indicate the previously published, less precise data for CF₃Cbl and CF₂HCbl. These are not included in the regression, but they indicate the improvement with the new data. The positive slope indicates that these cobalamins exhibit inverse trans influence. A similar plot for a larger number of cobalamins containing a Co–C bond, regardless of the precision of the axial distances, was reported with $r^2 = 0.919$ and equation Co–C = 0.649 Co–NB3 + 0.552.³⁵

The inverse trans influence is invariably reported for experimentally determined alkylcobalamins. However, it should be noted that DFT theoretical calculations of Co–C and Co–NB3 distances have indicated the possibility of normal trans influence in a series of structurally undetermined cobalamins having R groups with strong electron-withdrawing ability.⁴² Thus, inverse trans influence may not be a general feature of alkylcobalamins and may simply be limited by the structures thus far reported. In fact, the observation of normal or inverse trans influence most likely depends on a balance of steric and electronic properties of the R ligands, as has been observed for cobaloximes.⁴ Comparison of MeCbl and the new CF₃CH₂Cbl structure is of interest from this point-of-view. CF₃CH₂Cbl

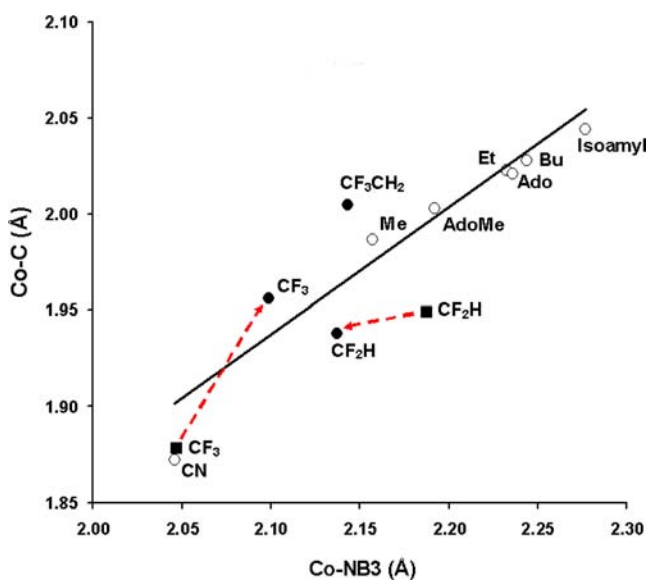


Figure 7. Plot of Co–C distances against Co–NB3 distances in alkylcobalamins and fluoroalkylcobalamins. The linear regression equation is $\text{Co–C} = 0.662 \text{ Co–NB3} + 0.548$, $r^2 = 0.850$ ($n = 10$). The fluoroalkylcobalamins reported in the present work are evidenced by filled circles. The previously reported less precise data for CF_3Cbl and CF_2HCbl , which are not included in the regression, are evidenced by filled squares. Further information on the structures included is given in Table S3.

could be considered an outlier in the plot of Figure 7. In fact, when compared with MeCbl , the tendency is that of normal trans influence. With respect to MeCbl , $\text{CF}_3\text{CH}_2\text{Cbl}$ has a smaller electron-donating ability and a larger bulk. The theoretical calculations predict normal trans influence in this scenario, and the data may therefore be seen as consistent with the theoretical prediction.⁴² If $\text{CF}_3\text{CH}_2\text{Cbl}$ is excluded from Figure 7, the correlation improves to $r^2 = 0.92$.

A number of structural correlations for cobalamins are considered in Figure 8. Details of the cobalamins considered are indicated in Table S3, which includes all of the reported structures of cobalamins with esd values $\leq 0.005 \text{ \AA}$ on Co–NB3 distance. It should be noted that different crystal structures of the same cobalamin are therefore present. It has previously been reported that the corrin fold angle (φ) is roughly correlated with the trans influence of the β -ligand, as measured by the Co–NB3 distance.⁴³ Although there is considerable scatter in the data, an increase of about 0.4 \AA in Co–NB3 length corresponds to a decrease of about 5° in φ .⁴³ Figure 8a shows this correlation with the present new data included. A rather poor linear correlation is obtained ($r^2 = 0.483$). This correlation quantifies the previous observation.⁴³ Clearly, the correlation only partially accounts for the variation observed. A previous report⁶ has suggested that crystal packing forces may also play a role. This possibility has been investigated in more recent investigations.^{44,45} DFT studies of coenzyme B_{12} by Rovira and Kozłowski⁴⁴ indicate that “the Co–Nax bond is largely influenced by crystal packing forces”, whereas Doyle et al.,⁴⁵ on the basis of comparison of five different CNCbl structures, concluded that random crystal packing effects are crucial in the solid state chemistry of Cbls. Figure 8b shows the variation of d , the out-of-plane displacement of the Co atom from the plane defined by the four equatorial nitrogen atoms, as a function of the Co–NB3

distance. A negative sign of d indicates displacement of the Co atom toward the β -ligand with respect to the four N donor atoms, whereas a positive sign indicates a relative displacement toward the NB3 fragment. A reasonably linear correlation is observed ($r^2 = 0.668$). Thus, as the Co–NB3 distance increases, which in turn is due to the increasing trans influence of the β -ligand, the relative shift of Co is toward the β -ligand. Finally, Figure 8c shows the variation of φ with d . In this case, the regression is rather poor ($r^2 = 0.425$), which again indicates that additional factors could influence the fold angle, as has been previously suggested.^{6,44,45}

Experimentally determined axial Co–X and Co–N distances (esd values $\leq 0.005 \text{ \AA}$) in XCbl and cobaloximes, $\text{pyCo}(\text{DH})_2\text{X}$, are reported in Table S4 for a series of X ligands. The regressions of Co–NB3 and Co–X₁ in XCbl against Co–py and Co–X₂ in $\text{pyCo}(\text{DH})_2\text{X}$, respectively, gave the following equations

$$\text{Co–X}_1 = 1.05 \text{ Co–X}_2 - 0.10, \quad r^2 = 0.943 \quad (1)$$

$$\text{Co–NB3} = 1.80 \text{ Co–py} - 1.54, \quad r^2 = 0.961 \quad (2)$$

The slope close to unity and the intercept close to zero in eq 1 indicate that the Co–X bond in cobalamins and cobaloximes responds in a similar way to steric and electronic effects (i.e., it is not significantly influenced by the equatorial moiety). On the contrary, the slope close to 2 in eq 2 indicates a much greater sensitivity of the Co–NB3 bond, with respect to that of Co–py, in responding to the trans influence of X, which is mediated by the equatorial ligand. Therefore, the axial Co–N bond shows evidence of cis influence of the equatorial moiety on the axial bond. Thus, these previously reported correlations are confirmed here for a series of X ligands showing a wider variety of electronic and steric characteristics.⁴

4.2. Relationship between Structure and Properties. It has been reported⁴ that the trend of the structural trans influence of the axial X ligand, measured by the Co–NB3 distance, is linearly related to the trend of the $\text{p}K_{\text{base-off}}$ for the base-on/base-off equilibrium (Scheme 1).⁴⁶ A linear relationship of $\text{p}K_{\text{base-off}}$ against the Co–NB3 distance with an r^2 value of 0.966 was found. The plot of Figure 9 shows that the three fluoroalkylcobalamins, the objects of the present study (evidenced by full circle in the plot), nicely fit that relationship when they are included in the linear regression ($r^2 = 0.963$). This is clear evidence that the structural trans influence follows the same trend of the thermodynamic trans influence.

Another established correlation in cobalamins is that between the ^{31}P NMR chemical shift of the phosphodiester nucleotide moiety (Figure 1) and the Co–NB3 distance (Table S5 and Figure S2).⁴⁷ A correlation factor of 0.84 was found for a series of cobalamins with X ranging from H_2O to NO and using Co–NB3 distances with esd values $\leq 0.01 \text{ \AA}$.⁴⁷ However, when the correlation is limited to Co–NB3 distances with esd values $\leq 0.005 \text{ \AA}$, the correlation factor slightly decreases to 0.82.⁴ In both cases, the point relative to NOCbl was dramatically out of the regression line. When NOCbl is excluded from the linear regression, the r^2 value increased to 0.94.⁴ The different behavior of $\text{p}K_{\text{base-off}}$ discussed above and the ^{31}P chemical shift with respect to the Co–NB3 distance was explained⁴ on the basis of the observation that the fraction of the base-off form in NOCbl solution is about 0.33.⁴⁸ In all of the other cobalamins included in the correlation, this fraction ranges from 2.0×10^{-8} ($\text{X} = \text{H}_2\text{O}$) to 0.047 ($\text{X} = \text{Et}$).⁴⁹ In the latter cobalamins, because there is significantly less base-off form fraction than in

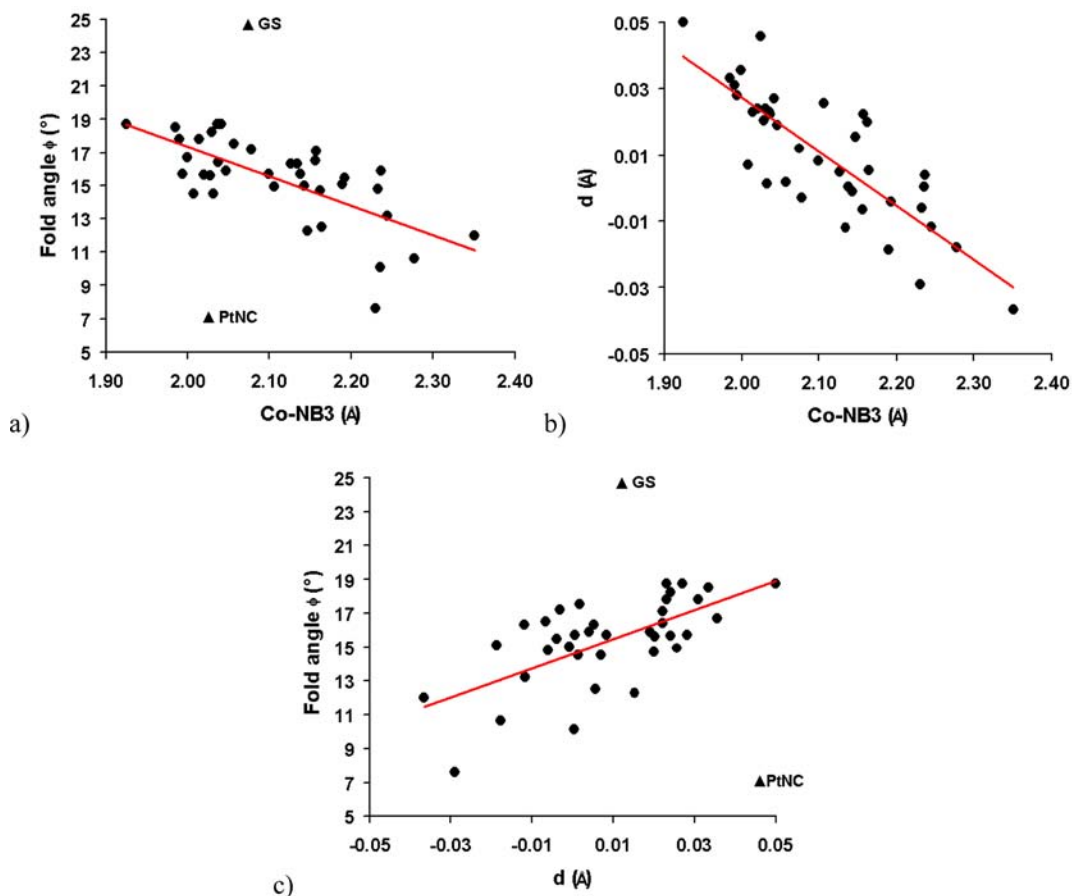
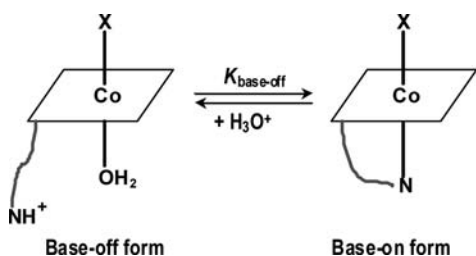


Figure 8. Plots of (a) the corrin fold angle (ϕ) against the Co–NB3 distance, (b) the Co displacement (d) from the plane of the N_{eq} donor atoms against the Co–NB3 distance, and (c) corrin fold angle (ϕ) against the Co displacement (d) from the plane of the N_{eq} donor atoms for cobalamins. The corresponding linear regression equations are $\phi = -17.677 \text{ Co-NB3} + 52.685$, $r^2 = 0.483$ ($n = 35$), $d = -0.163 \text{ Co-NB3} + 0.354$, $r^2 = 0.668$ ($n = 37$), and $\phi = 86.083 d + 14.63$, $r^2 = 0.425$ ($n = 35$). All of the cobalamin structures with esd values $\leq 0.005 \text{ \AA}$ on Co–NB3 distance were included in the linear regressions. Further information on the structures included is given in Table S3. (\blacktriangle) values for GlutathionylCbl (GS) and [enPtCl-vitB₁₂]⁺ (PtNC) are outliers excluded from the regression in plots a and c.

Scheme 1. Base-on/Base-off Equilibrium for Cobalamins



NOCbl, their ³¹P NMR signal is not affected by the fast exchange between base-on and base-off forms on the NMR time scale. On the contrary, the fast exchange between base-on and base-off forms of NOCbl affects its ³¹P NMR signal, which does not fit the regression well. Data relative to the present fluoralkylcobalamins fit well the above regressions, with the r^2 values being 0.81 and 0.92 (NOCbl excluded) when they are included in the regressions.

In the past, the detailed ¹³C NMR spectra of the benzimidazole moiety for several cobalamins, with X(R) varying from the very weak H₂O to the very strong electron donating *n*-Pr ligand, have been reported.^{10–12} It was suggested the inductive effects, related to the electron-donating ability of the axial ligand X(R), and Co anisotropy are important in

defining the trend in the ¹³C chemical shifts of the benzimidazole moiety. More recently, the ¹³C NMR spectrum of NOCbl and NO₂Cbl have become available.⁴⁸ In conjunction with the numerous Co–NB3 distances that are now also available, this allows a comparison between ¹³C chemical shifts and Co–NB3 distances, which essentially increase with the increase in the trans influencing ability of X(R). The relative chemical shifts of the benzimidazole C atoms (see Figure 1 for labeling scheme), together with the Co–NB3 distances (esd values $\leq 0.005 \text{ \AA}$) for several cobalamins with increasing donating ability of X(R), from H₂O to NO, are listed in Table S6. With the exceptions of B10, B11 (not shown), and B2 (Table S6), the ¹³C chemical shifts of the benzimidazole C atoms show significant variation with the increasing electron-donating ability of the axial ligand, from H₂O to NO. The difference in ¹³C chemical shift in the case of these two ligands, $\Delta(\text{NO-H}_2\text{O})$, is also indicated. The resonances of R1, B5, B6, and B7 move downfield, whereas those of R2, B8, B9, and B4 move upfield, as was previously reported for a smaller group of cobalamins.¹² Changes in B2 (Table S6), B10, and B11 resonances are small and erratic and do not appear to be related to the donating ability of X. Correlation factors from very good to fair are obtained for R1–R2 and B4–B9 chemical shifts with the Co–NB3 distances, as indicated in Table S6 and Figure S3. When NOCbl is excluded

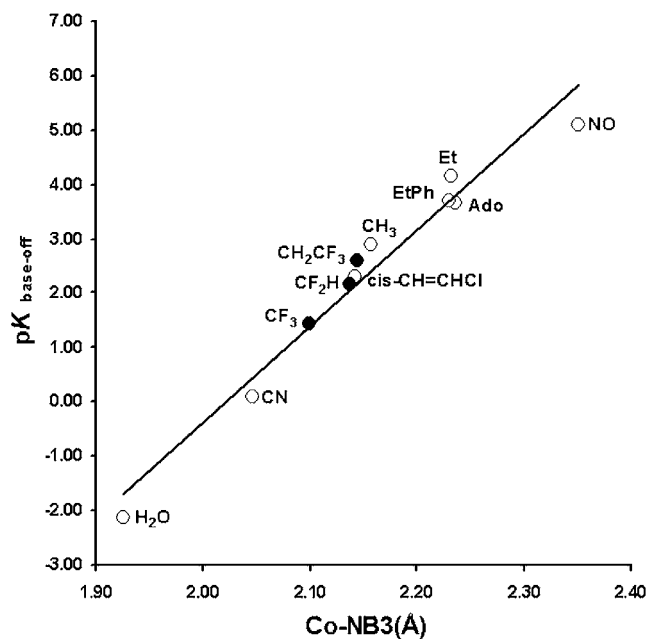


Figure 9. Plot of $\log K_{\text{base-off}}$ against Co–NB3 distances in cobalamins. The fluoroalkylcobalamins reported in the present work are evidenced by filled circles. Co–NB3 distances have esd values ≤ 0.005 Å. The equation of linear regression is $\log K_{\text{base-off}} = 17.713 \text{ Co-NB3} - 35.797$, $r^2 = 0.963$ ($n = 11$). $\log K_{\text{base-off}}$ values were taken from ref 1 except for NOCbl,⁴⁸ cis-ChlorovinylCbl (cis-CH=CHCl),⁵⁶ and EtPhCbl.¹⁷

from the regressions, because, as for ^{31}P chemical shifts discussed above, the significant presence of NOCbl base-off form may affect chemical shifts, the best correlations are for B5–B7 and R1. This analysis seems to suggest that the C resonances of the benzimidazole moiety, particularly those of B5–B7 and R1, which are from four to five bonds from Co and possibly less affected by the influence of Co anisotropy, are mainly influenced by inductive effects.

5. CONCLUSIONS

Two noteworthy findings emerge with regard to the crystal structures of the three fluoroalkylcobalamins examined in the present work ($\text{CF}_3\text{CH}_2\text{Cbl}$, CF_2HCbl , and CF_3Cbl). First, the previously unreported $\text{CF}_3\text{CH}_2\text{Cbl}$ exhibits a significant distortion of the axial fragment not only with respect to CF_2HCbl and CF_3Cbl but also with respect to EtCbl. This is attributed to steric effects. More significantly, comparison of the structures with those of their alkylcobalamin analogues with similar precision shows that the Co–C and Co–NB3 bond lengths are both shorter in fluoroalkylcobalamins. Previous literature reports were conflicting in this regard. This finding is attributed to the higher precision of the data reported here. Re-examination and updating of various correlations involving the electronic and steric influences of the β -ligand indicate that the fluoroalkylcobalamins exhibit a similar behavior to alkylcobalamins. In particular, the regression of out-of-plane displacement for the Co atom with respect to the Co–NB3 distance shows that the out-of-plane displacement of cobalt is mainly influenced by electronic effects of the β -ligand as well as the corrin fold angle.

■ ASSOCIATED CONTENT

§ Supporting Information

Crystallographic data for CF_2HCbl , CF_3Cbl , and $\text{CF}_3\text{CH}_2\text{Cbl}$ structures (data collection and refinement statistics and cif format); axial distances (Å) in $\text{LCo}(\text{chel})\text{R}$ and RCbl; structural features of cobalamins structures with Co–NB3 esd values ≤ 0.005 Å; axial distances in RCbl and $\text{pyCo}(\text{DH})_2\text{X}$; ^{31}P NMR resonances (ppm) of the phosphodiester nucleotide moiety and Co–NB3 distances for various cobalamins; ^{13}C NMR resonances (ppm) of the C atom of the benzimidazole moiety and Co–NB3 distances for various cobalamins; ^1H NMR spectra of CF_2HCbl , CF_3Cbl , and $\text{CF}_3\text{CH}_2\text{Cbl}$; plot of ^{31}P NMR resonances of the phosphodiester nucleotide moiety against Co–NB3 distances for various cobalamins; and plot of ^{13}C NMR resonances (ppm) of the benzimidazole moiety against Co–NB3 distances for various cobalamins. This material is available free of charge via the Internet at <http://pubs.acs.org>. The CCDC database code numbers 909997–909999 contain the supplementary crystallographic data for the CF_2HCbl , CF_3Cbl , and $\text{CF}_3\text{CH}_2\text{Cbl}$ structures. These data can be obtained free of charge via www.ccdc.cam.ac.uk/data_request/cif, by e-mailing data_request@ccdc.cam.ac.uk, or by contacting The Cambridge Crystallographic Data Center, 12 Union Road, Cambridge CB2 1EZ, United Kingdom; fax: +44 1223 336033.

■ AUTHOR INFORMATION

Corresponding Author

*Tel +39-040-5583936. Fax: +39-040-5583903. E-mail: sgeremia@units.it.

Present Address

[‡]Elettra — Sincrotrone Trieste, 34149 Basovizza — Trieste, Italy

Notes

The authors declare no competing financial interest.

■ ACKNOWLEDGMENTS

We thank MIUR (PRIN-2009A5Y3N project), CIRCMSB, FRA-2012 University of Trieste, and Friuli-Venezia-Giulia region (DPR. 120/2007/Pres.) for financial support and the XRD1 beamline scientists at the Elettra Synchrotron for technical assistance.

■ DEDICATION

[§]This work is dedicated to the memory of Professor L. Randaccio, who imagined and contributed to it but passed away before its completion.

■ REFERENCES

- (1) Brown, K. L. *Chem. Rev.* **2005**, *105*, 2075–2150.
- (2) Matthews, R. G. *Metal Ions in Life Sciences*; John Wiley & Sons: Chichester, U.K., 2009; Vol. 6.
- (3) Pratt, J. M. In *Chemistry and Biochemistry of B12*; Banerjee, R., Ed.; Wiley: New York, 1999.
- (4) De March, M.; Demitri, N.; Geremia, S.; Hickey, N.; Randaccio, L. *J. Inorg. Biochem.* **2012**, *116*, 215–227.
- (5) Schrauzer, G. N. *Acc. Chem. Res.* **1968**, *1*, 97–103.
- (6) Randaccio, L.; Geremia, S.; Nardin, G.; Wuerges, J. *Coord. Chem. Rev.* **2006**, *250*, 1332–1350.
- (7) Randaccio, L. *Comments Inorg. Chem.* **1999**, *21*, 327–376.
- (8) Randaccio, L.; Geremia, S.; Zangrando, E.; Ebert, C. *Inorg. Chem.* **1994**, *33*, 4641–4650.

- (9) Penley, M.; Brown, D.; Wood, J. *Biochemistry* **1970**, *9*, 4302–4310.
- (10) Brown, K. L.; Hakimi, J. M. *J. Am. Chem. Soc.* **1986**, *108*, 496–503.
- (11) Brown, K. L.; Satyanarayana, S. *J. Am. Chem. Soc.* **1992**, *114*, 5674–5684.
- (12) Calafat, A. M.; Marzilli, L. G. *J. Am. Chem. Soc.* **1993**, *115*, 9182–9190.
- (13) Hamza, M. S. A.; van Eldik, R. *Dalton Trans.* **2004**, 1–12.
- (14) Knight, J. C.; Edwards, P. G.; Paisey, S. J. *RSC Adv.* **2011**, *1*, 1415–1425.
- (15) Hattori, Y.; Asano, T.; Niki, Y.; Kondoh, H.; Kirihata, M.; Yamaguchi, Y.; Wakamiya, T. *Bioorg. Med. Chem.* **2006**, *14*, 3258–3262.
- (16) Siega, P.; Wuerges, J.; Arena, F.; Gianolio, E.; Fedosov, S. N.; Dreos, R.; Geremia, S.; Aime, S.; Randaccio, L. *Chem.—Eur. J.* **2009**, *15*, 7980–7989.
- (17) Ruetz, M.; Gherasim, C.; Gruber, K.; Fedosov, S.; Banerjee, R.; Kräutler, B. *Angew. Chem., Int. Ed.* **2013**, *52*, 2606–2610.
- (18) Wagner, T.; Afshar, C. E.; Carrell, H. L.; Glusker, J. P.; Englert, U.; Hogenkamp, H. P. C. *Inorg. Chem.* **1999**, *38*, 1785–1794.
- (19) Zou, X.; Brown, K. L. *Inorg. Chim. Acta* **1998**, *267*, 305–308.
- (20) Algarra, A. G.; Grushin, V. V.; MacGregor, S. A. *Organometallics* **2012**, *31*, 1467–1476.
- (21) Sgarbossa, P.; Scarso, A.; Strukul, G.; Michelin, R. A. *Organometallics* **2012**, *31*, 1257–1270.
- (22) Dubinina, G. G.; Brennessel, W. W.; Miller, J. L.; Vico, D. A. *Organometallics* **2008**, *27*, 3933–3938.
- (23) Rossi, M.; Glusker, J. P.; Randaccio, L.; Summers, M. F.; Toscano, P. J.; Marzilli, L. G. *J. Am. Chem. Soc.* **1985**, *107*, 1729–1738.
- (24) Brown, K. L.; Hakimi, J. M.; Nuss, D. M.; Montejano, Y. D.; Jacobsen, D. W. *Inorg. Chem.* **1984**, *23*, 1463–1471.
- (25) Kabsch, W. *Acta Crystallogr., Sect. D* **2010**, *66*, 125–132.
- (26) Leslie, A. G. W.; Powell, H. R. Processing diffraction data with mosflm. *Evolving Methods for Macromolecular Crystallography*; Springer: Dordrecht, The Netherlands, 2007; Vol. 245.
- (27) Evans, P. R. *Acta Crystallogr., Sect. D* **2006**, *62*, 72–82.
- (28) Winn, M. D.; Ballard, C. C.; Cowtan, K. D.; Dodson, E. J.; Emsley, P.; Evans, P. R.; Keegan, R. M.; Krissinel, E. B.; Leslie, A. G. W.; McCoy, A.; McNicholas, S. J.; Murshudov, G. N.; Pannu, N. S.; Potterton, E. A.; Powell, H. R.; Read, R. J.; Vagin, A.; Wilson, K. S. *Acta Crystallogr., Sect. D* **2011**, *67*, 235–242.
- (29) Burla, M. C.; Caliandro, R.; Camalli, M.; Carrozzini, B.; Cascarano, G. L.; De Caro, L.; Giacovazzo, C.; Polidori, G.; Siliqi, D.; Spagna, R. *J. Appl. Crystallogr.* **2007**, *40*, 609–613.
- (30) Sheldrick, G. M.; Schneider, T. R. SHELXL: High resolution refinement. In *Methods in Enzymology*; Academic Press: Orlando, FL, 1997; Vol. 277.
- (31) Emsley, P.; Cowtan, K. *Acta Crystallogr., Sect. D* **2004**, *60*, 2126–2132.
- (32) Parkin, S.; Moezzi, B.; Hope, H. *J. Appl. Crystallogr.* **1995**, *28*, 53–56.
- (33) Garau, G.; Geremia, S.; Marzilli, L. G.; Nardin, G.; Randaccio, L.; Tazher, G. *Acta Crystallogr., Sect. B* **2003**, *59*, 51–59.
- (34) Bresciani-Pahor, N.; Calligaris, M.; Randaccio, L.; Marzilli, L. G.; Summers, M. F.; Toscano, P. J.; Grossman, J.; Liotta, D. *Organometallics* **1985**, *4*, 630–636.
- (35) Hannibal, L.; Smith, C. A.; Smith, J. A.; Axhemi, A.; Miller, A.; Wang, S.; Brasch, N. E.; Jacobsen, D. W. *Inorg. Chem.* **2009**, *48*, 6615–6622.
- (36) Pratt, J. M. *Inorganic Chemistry of Vitamin B12*; Academic Press: New York, 1972.
- (37) Hensens, O. D., Hill, H. A. O., McClelland, C. E. In *B12*; Dolphin, D., Ed.; John Wiley & Sons: New York, 1982; Vol. 1.
- (38) Perry, C. B.; Fernandes, M. A.; Kenneth, L. B.; Zou, X.; Valente, E. J.; Marques, H. M. *Eur. J. Inorg. Chem.* **2003**, 2095–2107.
- (39) Stich, T. A.; Brooks, A. J.; Buan, N. R.; Brunold, T. C. *J. Am. Chem. Soc.* **2003**, *125*, 5897–5914.
- (40) Hill, H. A. O.; Pratt, J. M.; Williams, R. J. P. *Proc. R. Soc. London, Ser. A* **1965**, *288*, 352–358.
- (41) Randaccio, L.; Geremia, S.; Stener, M.; Toffoli, D.; Zangrando, E. *Eur. J. Inorg. Chem.* **2002**, 93–103.
- (42) Kuta, J.; Wuerges, J.; Randaccio, L.; Kozłowski, P. M. *J. Phys. Chem. A* **2009**, *113*, 11604–11612.
- (43) Randaccio, L.; Furlan, M.; Geremia, S.; Slouf, M.; Srnova, I.; Toffoli, D. *Inorg. Chem.* **2000**, *39*, 3403–3413.
- (44) Rovira, C.; Kozłowski, P. M. *J. Phys. Chem. B* **2007**, *111*, 3251–3257.
- (45) Marino, N.; Rabideau, A. E.; Doyle, R. P. *Inorg. Chem.* **2011**, *50*, 220–230.
- (46) Brown, K. L.; Hakimi, J. M.; Jacobsen, D. W. *J. Am. Chem. Soc.* **1984**, *106*, 7894–7899.
- (47) Hassanin, H. A.; El-Shahat, M. F.; DeBeer, S.; Smith, C. A.; Brasch, N. E. *Dalton Trans.* **2010**, *39*, 10626–10630.
- (48) Hassanin, H. A.; Hannibal, L.; Jacobsen, D. W.; Brown, K. L.; Marques, H. M.; Brasch, N. E. *Dalton Trans.* **2009**, 424–433.
- (49) Hamza, M.; Zou, X.; Brown, K.; van Eldik, R. *Inorg. Chem.* **2001**, *40*, 5440–5447.
- (50) Giannotti, C. In *B12*; Dolphin, D., Ed.; John Wiley & Sons: New York, 1982.
- (51) Mebs, S.; Henn, J.; Dittrich, B.; Paulmann, C.; Luger, P. *J. Phys. Chem. A* **2009**, *113*, 8366–8378.
- (52) Randaccio, L.; Furlan, M.; Geremia, S.; Slouf, M. *Inorg. Chem.* **1998**, *37*, 5390–5393.
- (53) Ouyang, L.; Rulis, P.; Ching, W.-Y.; Slouf, M.; Nardin, G.; Randaccio, L. *Spectrochim. Acta, Part A* **2005**, *61*, 1647–1652.
- (54) Kratky, C.; Faerber, G.; Gruber, K.; Wilson, K.; Dauter, Z.; Nolting, H.-F.; Konrat, R.; Kräutler, B. *J. Am. Chem. Soc.* **1995**, *117*, 4654–4670.
- (55) Randaccio, L.; Geremia, S.; Nardin, G.; Slouf, M.; Srnova, I. *Inorg. Chem.* **1999**, *38*, 4087–4092.
- (56) McCauley, K. M.; Pratt, D. A.; Wilson, S. R.; Shey, J.; Burkey, T. J.; van der Donk, W. A. *J. Am. Chem. Soc.* **2005**, *127*, 1126–1136.